Differential expression of miRNAs in Osborne's ligament of cubital tunnel syndrome

XIAN-HU ZHOU*, YI-MING REN*, ZHI-JIAN WEI*, WEI LIN, BAO-YOU FAN, SHEN LIU, YAN HAO, GUI-DONG SHI and SHI-QING FENG

Department of Orthopedics, Tianjin Medical University General Hospital, Tianjin 300052, P.R. China

Received March 8, 2016; Accepted February 20, 2017

DOI: 10.3892/mmr.2017.6663

Abstract. Cubital tunnel syndrome (CuTS) is the second most common peripheral nerve compression disease, however, the pathogenesis and pathology of CuTS remain to be fully elucidated. The aim of the present study was to compare the expression pattern of microRNAs (miRNAs) in pachyntic Osborne's ligament with that in control tendinous tissue, and select meaningful miRNAs for further investigation of the clinical pathological mechanism underlying CuTS. A microarray assay was performed to examine the expression profiles of miRNAs in the Osborne's ligament and control tendinous tissues. An online bioinformatics algorithms tool (miRWalk) was used to predict putative target genes for the deregulated miRNAs, and functional annotation was performed by Gene Ontology (GO) enrichment and Kyoto Encyclopedia of Genes and Genomes (KEGG) pathway analysis. Finally, the results of microarray were partially validated using reverse transcription-quantitative polymerase chain reaction analysis. The expression of total of 60 miRNAs were found to be significantly different between the pachyntic Osborne's ligament and control tendinous tissues. MiRWalk2.0 predicted 1,804 target genes for these miRNAs, and the GO functional analysis of the predicted genes suggested cellular mechanisms, including metabolic process, regulation of cell growth, cell cycle processes, cell division regulation, cellular metabolic process and signal transmission, were involved. Furthermore, KEGG pathway analysis revealed important pathways, including adherent junction, focal adhesion, lysine degradation, cell adhesion molecules and mitogen-activated protein kinase. Compared with the heathy tissue, Osborne's ligament tissue from patients with CuTS showed a markedly different miRNA expression profile, which suggested that miRNAs may be involved in the pathogenesis of CuTS.

Correspondence to: Dr Shi-Qing Feng, Department of Orthopedics, Tianjin Medical University General Hospital, 154 Anshan Road, Heping, Tianjin 300052, P.R. China
E-mail: sqfeng@tmu.edu.cn

*Contributed equally

Key words: cubital tunnel syndrome, Osborne's ligament, microRNA, microarray, Kyoto Encyclopedia of Genes and Genomes

Introduction

Cubital tunnel syndrome (CuTS), also known as delayed ulnar neuritis, is the second most common peripheral nerve compression disease in the upper limb following carpal tunnel syndrome (1). It is estimated that 25 per 100,000 individuals are affected by CuTS in Italy each year, and is two times more common in men, compared with women (2). CuTS can occur as a result of ischemia or mechanical compression by repeated elbow flexion, post-traumatic scarring, anomalous musculature or direct compression, although the exact cause may be difficult to identify (3). Early symptoms in patients can include elbow discomfort, numbness of the little finger, and inflexibility when writing or using tools. In more severe forms of CuTS, the strength of the flexor carpi ulnaris, and flexor muscles of the ring and little fingers are weakened; atrophy of the intrinsic muscle of the hand and mild claw finger deformity can also occur (4). Treatment methods include non-surgical therapies, for example rest, splinting, real-time visualized ultrasound-guided injection and surgical decompression, which can include open *in situ* decompression, anterior transposition and endoscopic decompression (5-8).

At present, investigations of CuTS are focused predominantly on surgical methods, and less on the discussion of pathogenesis and pathology. Although ulnar nerve compression is a common cause of CuTS, its pathogenesis and pathology remain to be fully elucidated. The common areas of entrapment of the ulnar nerve include the arcade of Struthers, the medial intermuscular septum, insertion of the medial head of the triceps, the leading edge of the cubital tunnel retinaculum, and the anconeus epitrochlearis muscle, medial epicondyle, Osborne's ligament and flexor-pronator group. Hypertrophy of Osborne's ligament is an important cause of ulnar nerve compression (9).

Extensive investigations have been performed to characterize the differences between healthy and diseased ligaments, including alterations in gene expression. MicroRNAs (miRNAs), defined as endogenously expressed, short non-coding RNAs (18-25 nucleotides in length), suppress protein translation through binding to target messenger RNAs (mRNAs). They are expressed at specific stages of tissue

development or cell differentiation, and have marked effects on the expression of a variety of genes at the post-transcriptional stage (10).

Previous studies have suggested that miRNAs contribute to the pathogenesis of fibrotic diseases. Hypertrophy of the ligamentum flavum (LF) is crucial in lumbar spinal stenosis (LSS) and is caused primarily by fibrosis. miRNA (miR)-155 is positively correlated with different fibrotic diseases. Previous data have shown that the expression levels of miR155 differ between LF and LSS groups, and between LF and lumbar disc herniation (LDH) groups. Therefore, the fibrosis-associated miR-155 may be important in the pathogenesis of hypertrophic LF (11). However, the role of miRNAs in the development of hypertrophy of the ligaments remains to be elucidated.

To improve understanding of the pathogenesis of CuTS, the present collected examined pachyntic Osborne's ligaments and control tendinous tissues. Global miRNA expression levels in the pachyntic Osborne's ligaments and control tendinous tissues were examined using microarray techiques. The results showed differences in miRNAs expression levels between the Osborne's ligament and control tendinous tissues from patients with CuTS. These findings have important implications for revealing the pathogenesis of CuTS.

Materials and methods

Patients and tissue samples. The patients included in the present study comprised six patients with CuTS, which was diagnosed according to their symptoms, neurological examination, electrophysiological examination and imaging. The patients all experienced numbness of the little finger and the ring finger, pain in the elbow and forearm, weakness and clumsiness of the hand and motor deficit, including Froment's sign. X-ray imaging of the positive and lateral position of the elbow joint, tangential position of the ulnar nerve, conventional assay and ECG were included in the basic examination. Reductions in the velocity of motor nerve conduction in the patient elbow segments were identified by electromyography. Local color Doppler ultrasound was used to exclude elbow tumor lesions.

The Osborne's ligament and control tendinous tissue samples were obtained from four men and two women with CuTS (average age, 53.83 years; range, 31-76 years) who underwent surgery for anterior subcutaneous transposition. Detailed characteristics for the patients are shown in Table I. During surgery, an arched 6-8 cm incision with a tourniquet control was made posterior to the medial epicondyle. The retrocondylar groove, Osborne's ligament and ulnar nerve were identified. Proximally, the ulnar nerve was exposed to the medial intermuscular septum, which was divided to avoid possible future compression. Following division and transection of the Osborne's ligament from the cubital tunnel retinaculum, the ulnar nerve was released distally to the two heads of the flexor carpi ulnaris. Soft loops were used to isolate the ulnar nerve, and the ulnar nerve was transposed forward to the medial epicondyle. To stabilize the ulnar nerve, the subcutaneous tissue was sutured using a fascial flap. As medical waste, the Osborne's ligaments were collected. In addition ~0.3x1 cm tendinous tissue around the two heads of the flexor carpi ulnaris was excised as a control sample. The specimens wesre collected by the same experienced surgeon in the Department of Orthopedics of Tianjin Medical University General Hospital (Tianjin, China). The Tianjin Medical University General Hospital Medical Ethics Committee approved the consent forms and protocol for evaluating the tissues. Written informed consent was provided by each patient prior to surgery. The specimens were frozen in liquid nitrogen and stored at -80˚C until the microarray was performed.

RNA isolation. Three groups of stored samples were assayed using an Affymetrix GeneChip 3000 TG system purchased from Affymetrix, Inc. (Santa Clara, CA, USA). First frozen samples were homogenized in QIAzolLysis Reagent (Qiagen GmbH, Hilden, Germany) using the TissueRuptor. Total RNA was precipitated using chloroform and the aqueous phase was mixed with 1.5 volumes of 100% Ethanol. Then total RNA, including miRNAs, was extracted using TRIzol reagent (Invitrogen; Thermo Fisher Scientific, Inc., Waltham, MA, USA) according to the manufacturer's protocol. The concentration of RNA was measured using a NanoDrop ND-2000 spectrophotometer (NanoDrop; Thermo Fisher Scientific, Inc., Wilmington, DE, USA), and the purity of RNA was confirmed using spectrophotometry. The optical density 260/280 nm ratio was between 1.90 and 2.10 for each RNA sample.

Microarray hybridization and data analysis. The RNA quality was assessed using denaturing gel electrophoresis. The Affymetrix GeneChip system was used for hybridization, staining and imaging of the arrays, according to the standard Affymetrix protocol. Following hybridization, the arrays were washed using a Fluidics Station 450 (Affymetrix; Thermo Fisher Scientific Inc.) and then scanned using a Scanner 3000 7G 4C (Affymetrix; Thermo Fisher Scientific Inc.). Quality control analysis was performed using the Affymetrix miRNA QCTool (Affymetrix; Thermo Fisher Scientific Inc.). For each miRNA, multiple probes were spotted on the array, and the mean intensity of these probes was calculated to represent the expression value of the miRNAs. In addition, multiple spots were included as negative controls. For each sample, 1 μl total RNA was hybridized with the miRNA array and further processed in accordance with the manufacturer's protocol. Only those miRNAs with significant ($P<0.05$) differential expression of ≥2.0-fold change were reported. Array scanning and data analysis were performed using Expression Console™ software version 1.4 (Affymetrix; Thermo Fisher Scientific Inc.), which provides signal estimation and quality control functionality for the Affymetrix GeneChip and Transcriptome Analysis Console software version 1.0 (Affymetrix; Thermo Fisher Scientific Inc.), which performs statistical analysis and provides a list of differentially expressed miRNAs. miRWalk2.0 (http://www.umm.uni-heidelberg.de/apps/zmf/mirwalk/) (12) was used synthesizing four existing miRNA-target prediction programs (miRanda, miRDB, TargetScan and RNA22), as the commonly used web tools for bioinformatics algorithms, to identify the potential targets of those miRNAs by combined analysis of the mRNAs in the whole genome expression microarray. The Bioconductor gene annotation tool version 3.4 (http://www.bioconductor.org) was used to perform Gene Ontology (GO) function and Kyoto Encyclopedia of Genes and Genomes (KEGG) pathway analysis. A Venn diagram was produced to show the potential common significant GO terms

Table I. Characteristics of patients.

Characteristic	Patient 1	Patient 2	Patient 3	Patient 4	Patient 5	Patient 6
Gender	Male	Female	Male	Male	Female	Male
Age (years)	61	76	64	53	31	38
Surgical method	ASCT	ASCT	ASCT	ASCT	ASCT	ASCT
Side of surgery	Left	Right	Right	Bilateral	Left	Left
Surgery on dominant side	No	Yes	Yes	Yes	No	No
Electromyography	Positive	Positive	Positive	Positive	Positive	Positive
Tinel's sign	Positive	Positive	Positive	Positive	Positive	Positive
Sample application	Microarray	Microarray	Microarray	RT-qPCR	RT-qPCR	RT-qPCR

ASCT, anterior subcutaneous transposition; RT-qPCR, reverse transcription-quantitative polymerase chain reaction.

Table II. Primers used for reverse transcription-quantitative polymerase chain reaction analysis.

miRNA	miRNA sequence (5'-3')	Primer sequence (5'-3')	Primer length (bp)	GC content (%)	Tm (˚C)
hsa-miR-21-3p	CAACACCAGUCGAUGGGCUGU	Forward ATT CAA CAC CAG TCG ATG GGC Reverse TAG CTT ATC AGA CTG ATG TT	21	52	60.2
hsa-miR-146b-5p	UGAGAACUGAAUUCCAUAGGCU	Forward GTG AGA ACT GAA TTC CAT AGG CT Reverse GCA CCA GAA CTG AGT CCA CA	23	43	59.9
hsa-miR-1343-3p	CUCCUGGGGCCCGCACUCUCGC	Forward TTA TTC TCC TGG GGC CCG C Reverse ATC CCA CCA CTG CCA CC	19	63	60.6

miR/miRNA, microRNA.

among the five miRNAs (hsa-miR-146b-5p, hsa-miR-21-3p, hsa-miR-185-3p, hsa-miR-615-5p and hsa-miR-663a), which included the majority of the predicted target genes.

Reverse transcription-quantitative polymerase chain reaction (RT-qPCR) analysis. In total, three miRNAs were identified with significant differences, one differentially upregulated (hsa-miR-1343-3p) and two differentially downregulated (hsa-miR-21-3p and hsa-miR-146b-5p). These three miRNAs were verified using RT-qPCR analysis with the Bio-Rad CFX96 Real-Time PCR system (Bio-Rad Laboratories, Inc., Hercules, CA, USA). Total RNA was isolated from the samples of the other three patients with CuTS using TRIzol (Invitrogen; Thermo Fisher Scientific, Inc.), and this was polyadenylated and reverse-transcribed with a poly (T) adapter into cDNA by miScript Reverse Transcription kit (Qiagen GmbH) according to the manufacturer's protocol. Then qPCR was performed using SYBR green dye in a thermal cycler with the following parameters: 1 μl buffer, 4 μl total RNA, 2 μl cDNA, 1 μl specific primers, 4 μl RNase-free water and 10 μl SYBR qPCR Mix. An initial denaturation step at 95˚C for 30 min; 40 cycles at 95˚C for 5 sec and 60˚C for 30 sec. The complete experimental procedure was performed for each sample in triplicate. All primers were synthesized by Shanghai Shenggong Biology Engineering Technology Service, Ltd. (Shanghai, China) and the miRNA-specific primers are listed in Table II. All data were analyzed using the $2^{-\Delta\Delta Cq}$ method (13) to calculate the differences between the quantification cycle values of the target genes in each sample. $P<0.05$ was considered to indicate a statistically significant difference.

Statistical analysis. All data were analyzed using SPSS statistical software (version 11.5 for Windows; SPSS, Inc., Chicago, IL, USA). Statistical analysis was performed using two-tailed Student's *t*-test. $P<0.05$ was considered to indicate a statistically significant difference.

Results

Expression profile of miRNAs in the ligament. To investigate the miRNA expression profiles in the pachyntic Osborne's ligament, microarray analysis was performed using total RNA from pachyntic Osborne's ligaments and control tendinous tissues obtained from patients with CuTS. The expression levels of 60 miRNAs showed significant differential expression between the pachyntic Osborne's ligament group and the control group (Fig. 1). Among these, only three miRNAs were upregulated, whereas the remaining 67 were downregulated (Table III).

Prediction of miRNA target genes and functional analysis. To elucidate the functionality of the regulated miRNAs, miRNA gene target prediction was performed for the 60 differentially expressed miRNAs using the online freely available software, miRWalk2.0. A total of 1,804 predicted target genes of the three upregulated miRNAs and 67 downregulated miRNAs were found, respectively. Functional annotation of the major target genes were from seven miRNAs (hsa-miR-146b-5p, hsa-miR-21-3p, hsa-miR-185-3p, hsa-miR-615-5p, hsa-miR-659-3p, hsa-miR-663a and hsa-miR-760), which were analyzed by GO enrichment analysis to further evaluate the biological implications of the differentially expressed miRNAs. The possible regulatory pathways of the major target genes were analyzed based on KEGG pathway terms. The GO categories included protein metabolic process, regulation of cell growth, cell cycle process, regulation of cell division, cellular metabolic process and signal transmission. The Venn diagram, which was constructed using the Bioconductor tool, showed that there were certain common significant GO terms among the different miRNAs (Fig. 2). According to the analysis of enriched KEGG pathways for the targets identified from the differentially expressed miRNAs, the predicted target genes of the differentially expressed miRNAs were associated with adherent junction, focal adhesion, axon guidance, lysine degradation, other glycan degradation, cell adhesion molecules (CAMs), mitogen-activated protein kinase (MAPK) signaling pathway, retrograde endocannabinoid signaling, ErbB signaling pathway, glycosaminoglycan biosynthesis-heparin sulfate/heparin and neurotrophic signaling pathway (Table IV). KEGG pathway analysis revealed a number of underlying biological processes, which may be involved in pachynsis of Osborne's ligament and may provide useful clues for further investigating the miRNA targets.

Validation of miRNA expression by RT-qPCR analysis. In addition to validating the microarray results, RT-qPCR was used to quantify particular miRNAs in the pachyntic Osborne's ligament, including the one differentially upregulated miRNA (hsa-miR-1343-3p) and two differentially downregulated miRNAs (hsa-miR-21-3p and hsa-miR-146b-5p), which were closely associated with fibrotic disease following the online database search. As shown in Fig. 3, the expression patterns of hsa-miR-1343-3p, hsa-miR-21-3p and hsa-miR-146-5p detected using RT-qPCR were consistent with the microarray data, with significance ($P<0.05$).

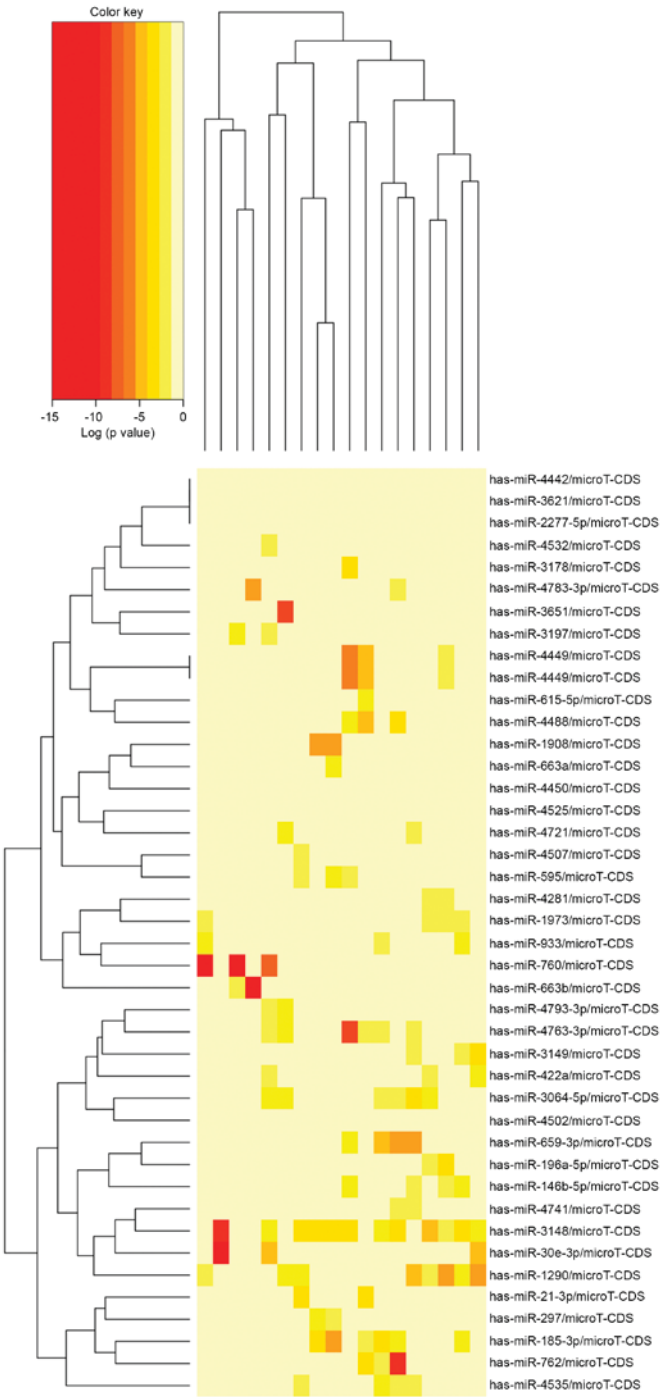

Figure 1. Heat map and unsupervised hierarchical cluster analysis of the differentially expressed miRNAs in pachyntic Osborne's ligament groups and control tendinous tissue groups. Columns and rows represent samples and specific miRNAs. The samples were grouped together into the pachyntic Osborne's ligament group and control tendinous tissue group, according to their expression pattern. The miRNA clustering tree is shown on the left. The color scale shows the relative expression level of miRNAs as the log (P-value) -transformed values. Red indicates that the miRNA shows markedly different expression in the pachyntic Osborne's ligament group, compared with that in the control; yellow indicates less difference in the expression of miRNA between the pachyntic Osborne's ligament and control groups. miRNA/miR, microRNA.

Discussion

In the present study, the patients examined were all engaged in heavy physical work. Chronic repetitive strain can cause

Table III. Summary of the significantly differentially expressed miRNAs.

miRNA	logFC (fold change)	P-value	Sequence (5'-3')
Upregulated			
hsa-miR-7855-5p	1.045103351	0.000425931	UUGGUGAGGACCCCAAGCUCGG
hsa-miR-422a	1.377981007	0.000219629	ACUGGACUUAGGGUCAGAAGGC
hsa-miR-1343-3p	0.934668054	0.000311621	CUCCUGGGGCCCGCACUCUCGC
Downregulated			
hsa-miR-196a-5p	-6.520640993	0.000000057	UAGGUAGUUUCAUGUUGUUGGG
hsa-miR-1290	-3.225990914	0.000000895	UGGAUUUUUGGAUCAGGGA
hsa-miR-595	-3.859379525	0.000001060	GAAGUGUGCCGUGGUGUGUCU
hsa-miR-7110-5p	-3.949821874	0.000006230	UGGGGGUGUGGGGAGAGAGAG
hsa-miR-3148	-2.477794005	0.000006770	UGGAAAAAACUGGUGUGUGCUU
hsa-miR-4532	-3.334823954	0.000008990	CCCCGGGGAGCCCGGCG
hsa-miR-3064-5p	-3.049176967	0.000009880	UCUGGCUGUUGUGGUGUGCAA
hsa-miR-6792-5p	-1.989451562	0.000010600	GUAAGCAGGGGCUCUGGGUGA
hsa-miR-7844-5p	-2.838409598	0.000017300	AAAACUAGGACUGUGUGGUGUA
hsa-miR-4535	-2.017418576	0.000018300	GUGGACCUGGCUGGGAC
hsa-miR-146b-5p	-5.085472937	0.000020700	UGAGAACUGAAUUCCAUAGGCU
hsa-miR-3178	-2.277544498	0.000022100	GGGGCGCGGCCGGAUCG
hsa-miR-297	-4.106551942	0.000028200	AUGUAUGUGUGCAUGUGCAUG
hsa-miR-21-3p	-3.565524376	0.000037100	CAACACCAGUCGAUGGGCUGU
hsa-miR-4525	-3.485981804	0.000052800	GGGGGGAUGUGCAUGCUGGUU
hsa-miR-6789-5p	-1.746637528	0.000054700	GUAGGGGCGUCCCGGGCGCGCGGG
hsa-miR-6883-5p	-2.808853491	0.000061600	AGGGAGGGUGUGGUAUGGAUGU
hsa-miR-3149	-1.879048778	0.000066500	UUUGUAUGGAUAUGUGUGUGUAU
hsa-miR-4502	-2.622259256	0.000070000	GCUGAUGAUGAUGGUGCUGAAG
hsa-miR-933	-1.918951061	0.000081100	UGUGCGCAGGGAGACCUCUCCC
hsa-miR-4793-3p	-3.351094169	0.000084600	UCUGCACUGUGAGUUGGCUGGCU
hsa-miR-6085	-1.483750019	0.000085000	AAGGGGCUGGGGGAGCACA
hsa-miR-760	-1.736503688	0.000086000	CGGCUCUGGGUCUGUGGGGA
hsa-miR-6075	-2.645791301	0.000090600	ACGGCCCAGGCGGCAUUGGUG
hsa-miR-4741	-1.682786276	0.000096200	CGGGCUGUCCGGAGGGGUCGGCU
hsa-miR-6875-5p	-3.198242537	0.000102689	UGAGGGACCCAGGACAGGAGA
hsa-miR-6845-5p	-2.537516128	0.000110628	CGGGGCCAGAGCAGAGAGC
hsa-miR-1180-3p	-3.290772167	0.000120042	UUUCCGGCUCGCGUGGGUGUGU
hsa-miR-3620-5p	-1.269433220	0.000125189	GUGGGCUGGGCUGGGCUGGGCC
hsa-miR-663a	-1.826255642	0.000153410	AGGCGGGGCGCCGCGGGACCGC
hsa-miR-663b	-3.478527017	0.000155267	GGUGGCCCGGCCGUGCCUGAGG
hsa-miR-3621	-1.444956668	0.000161666	CGCGGGUCGGGGUCUGCAGG
hsa-miR-4721	-3.187701938	0.000188641	UGAGGGCUCCAGGUGACGGUGG
hsa-miR-6791-5p	-1.769619706	0.000205615	CCCCUGGGGCUGGGCAGGCGGA
hsa-miR-1973	-1.699316842	0.000233469	ACCGUGCAAAGGUAGCAUA
hsa-miR-659-3p	-1.301640751	0.000244329	CUUGGUUCAGGGAGGGUCCCCA
hsa-miR-4507	-1.921339340	0.000257577	CUGGGUUGGGCUGGGCUGGG
hsa-miR-6740-5p	-2.050797179	0.000259650	AGUUUGGGAUGGAGAGAGGAGA
hsa-miR-6816-5p	-1.940639258	0.000282808	UGGGGCGGGGCAGGUCCCUGC
hsa-miR-6836-5p	-3.707920585	0.000310829	CGCAGGGCCCUGGCGCAGGCAU
hsa-miR-185-3p	-2.848826390	0.000322188	AGGGGCUGGCUUUCCUCUGGUC
hsa-miR-4763-3p	-1.844484822	0.000334158	AGGCAGGGGCUGGUGCUGGGCGGG
hsa-miR-30e-3p	-1.602759453	0.000335463	CUUUCAGUCGGAUGUUUACAGC
hsa-miR-1237-5p	-1.676336572	0.000348059	CGGGGGCGGGGCCGAAGCGCG
hsa-miR-6084	-1.326538904	0.000356453	UUCCGCCAGUCGGUGGCCGG
hsa-miR-4488	-1.219288223	0.000357825	AGGGGGCGGGCUCCGGCG
hsa-miR-4450	-2.075168762	0.000360412	UGGGGAUUUGGAGAAGUGGUGA

Table III. Continued.

miRNA	logFC (fold change)	P-value	Sequence (5'-3')
hsa-miR-3651	-4.214617171	0.000361525	CAUAGCCCGGUCGCUGGUACAUGA
hsa-miR-4449	-4.741198585	0.000393060	CGUCCCGGGGCUGCGCGAGGCA
hsa-miR-762	-1.666761846	0.000444374	GGGGCUGGGGCCGGGGCCGAGC
hsa-miR-6765-5p	-1.765624284	0.000463632	GUGAGGCGGGGCCAGGAGGGUGUGU
hsa-miR-2277-5p	-0.827734961	0.000465336	AGCGCGGGCUGAGCGCUGCCAGUC
hsa-miR-3197	-5.698464480	0.000488920	GGAGGCGCAGGCUCGGAAAGGCG
hsa-miR-615-5p	-3.033691421	0.000502284	GGGGGUCCCCGGUGCUCGGAUC
hsa-miR-4783-3p	-2.084261251	0.000519843	CCCCGGUGUUGGGGCGCGUCUGC
hsa-miR-1343-5p	-1.042812782	0.000541584	UGGGGAGCGGCCCCCGGGUGGG
hsa-miR-6815-5p	-2.100053152	0.000542802	UAGGUGGCGCCGGAGGAGUCAUU

miR, microRNA.

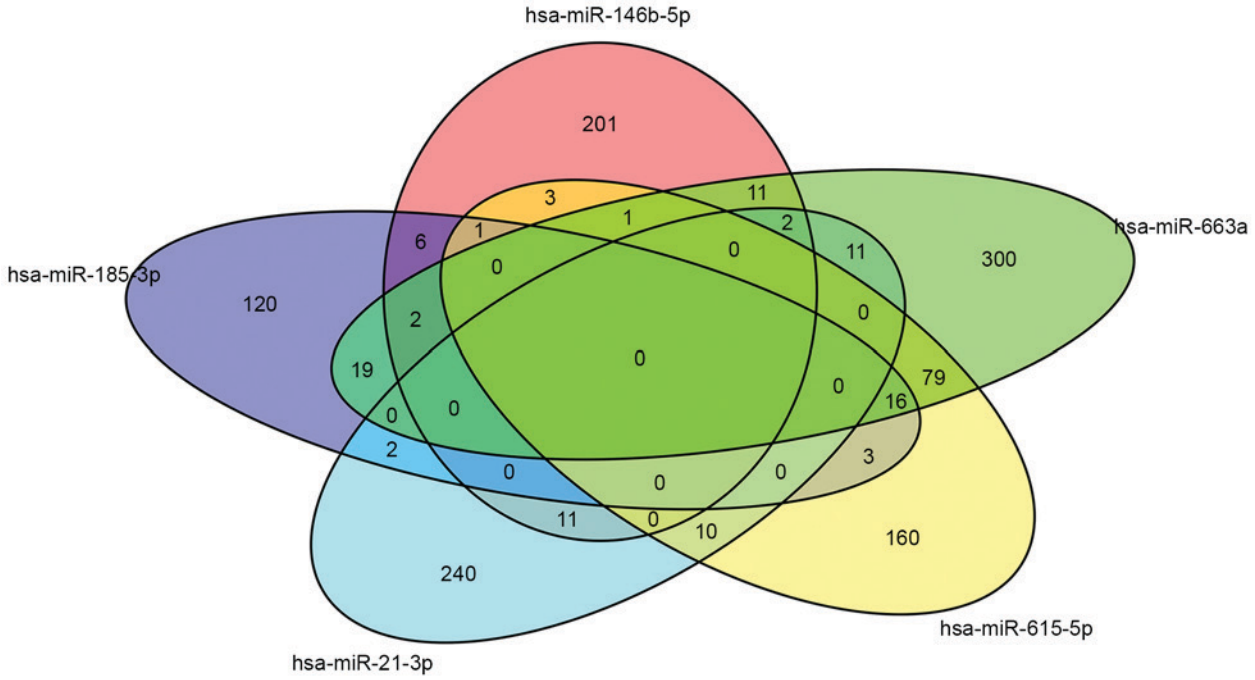

Figure 2. Venn diagram of five miRNAs, including the majority of the predicted target genes. The Venn diagram shows the potential common significant GO terms among five miRNAs (hsa-miR-146b-5p, hsa-miR-21-3p, hsa-miR-185-3p, hsa-miR-615-5p and hsa-miR-663a), which include the majority of the predicted target genes. Different colors represent different miRNAs. The number in the intersection represents the number of common GO terms among the miRNAs. GO, Gene Ontology; miRNA/miR, microRNA.

hypertrophy of Osborne's ligament in the cubital tunnel, and lead to compression of the ulnar nerve and degenerative ulnar neuritis, which is the most common etiology of CuTS. Naran and Imbriglia (14) showed that 55% of patients engaged in activities, which placed repetitive strain or compression on the ulnar nerve, and 48% percent of patients worked as heavy manual laborers in the population demographics. Another study indicated that the incidence of ulnar nerve entrapment at the elbow was associated with one biomechanical risk factor, which was repetitively holding a tool in position (15). Although several other factors, including cubitus valgus, anomalous musculature and direct compression, can also lead to CuTS, the present study focused on the molecular pathogenesis of degenerative ulnar neuritis triggered by hypertrophy of Osborne's ligament (4).

Emerging evidence has demonstrated that dysregulation of miRNAs may contribute to the etiology and pathophysiology of fibrosis and scarring, For example, miR-155 is a fibrosis-associated miRNA, which increases the expression of collagen I and collagen III in fibroblasts, and may be involved in the pathogenesis of LF hypertrophy (11). The inhibition of miR-145 assists in preventing or reducing hypertrophic scarring of the skin by reducing skin myofibroblast activity, and decreasing the expression of α1 type I collagen and secretion

Table IV. KEGG pathway analysis for the predicted miRNA targets.

KEGG pathway	P-value	Genes (n)	miRNAs (n)
Prion diseases	0.000000	3	2
Systemic lupus erythematosus	0.000000	31	3
Alcoholism	0.000000	39	4
Adherens junction	0.000000	30	9
Axon guidance	0.000000	51	9
Other glycan degradation	0.000003	3	2
Lysine degradation	0.000111	19	9
Transcriptional misregulation in cancer	0.000165	65	9
Cell adhesion molecules	0.000215	23	8
Mitogen-activated protein kinase signaling pathway	0.000567	86	8
ErbB signaling pathway	0.005328	29	8
Circadian entrainment	0.007704	35	6
Neurotrophin signaling pathway	0.017656	47	7
Prostate cancer	0.01956	32	5
Focal adhesion	0.025566	67	7
Long-term potentiation	0.032181	25	6
Retrograde endocannabinoid signaling	0.032885	33	4
Glycosaminoglycan biosynthesis-heparan sulfate/heparin	0.041110	8	6

miRNA, microRNA; KEGG, Kyoto Encyclopedia of Genes and Genomes.

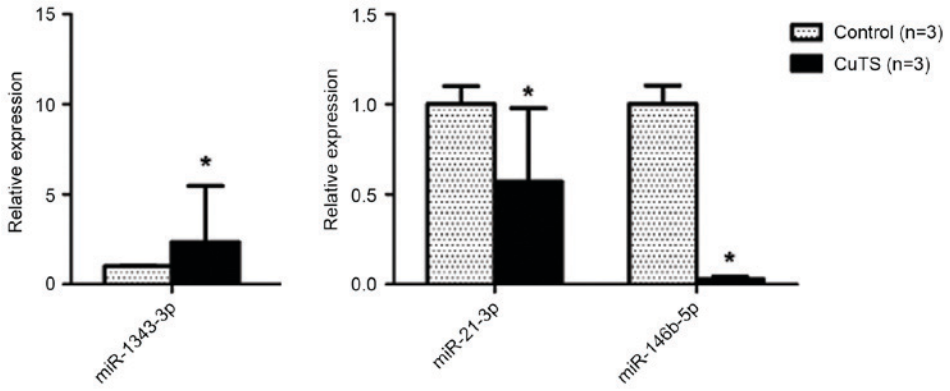

Figure 3. Validation of the differential expression of the three miRNAs identified in the microarray using RT-qPCR. RT-qPCR was used to analyze the expression of miR-1343-3p, miR-21-3p and miR-146b-5p in Osborne's ligaments from patients with CuTS. Data indicate the relative expression following normalization and values are presented as the mean ± standard error of the mean. *P<0.05, vs. control. miRNA/miR, microRNA; CuTS group, pachyntic Osborne's ligament tissues from patients with cubital tunnel syndrome; control group, control tendinous tissues from patients with cubital tunnel syndrome; RT-qPCR, reverse transcription-quantitative polymerase chain reaction.

of transforming growth factor-β1 (TGF-β) (16). miRNA-21 regulates systemic sclerosis fibrosis via directly targeting TGF-β signaling (17). miR-200b, which regulates the proliferation and apoptosis of human hypertrophic scar fibroblasts, has previously been reported to be associated with hypertrophic scarring by affecting the synthesis of collagen I and III, the expression of fibronectin, and TGF-β1/α-smooth muscle actin signaling (18). However, few studies have examined the effects of miRNAs in hypertrophy of Osborne's ligament.

In the present study, the miRNA expression profiles showed differentially expressed miRNAs in pachyntic Osborne's ligaments and control tendinous tissues of patients with CuTS, identifying miRNAs and the downstream signaling pathway involved in the mechanism of hypertrophy of Osborne's ligament. In total, three upregulated and 67 downregulated miRNAs were found. The three miRNAs (hsa-miR-1343-3p, hsa-miR-21-3p and hsa-miR-146b-5p) were verified using RT-qPCR analysis, and their expression patterns were in accordance with the microarray data, with significance (P<0.05). These miRNAs have been reported in other fields of investigation. miR-146b-5p and let-7f were validated as miRNA markers differentiating papillary thyroid cancer from other clinical conditions (19). In solid tumors, miR-146b-5p is frequently downregulated, including in prostate cancer,

pancreatic cancer and glioblastoma; in glioblastoma cell lines, miR-146b-5p is overexpressed, leading to the silencing of matrix metalloproteinase (MMP) 16 mRNA, inactivation of MMP2, and inhibition of tumor cell migration and invasion (20). Another finding suggested that miR-146b-5p may be associated with pancreatic cancer cell migration and invasion by MMP16, which is a downstream target of miR-146b-5p (21). Osborne's ligament is a well-defined fibrous band, which consists of connective tissue cells within collagen fibrils (22). Hypertrophy of Osborne's ligament may be associated with abnormal variations of elastic and collagen fibers. MMPs, a large family of endopeptidases, are involved in tissue remodeling and the degradation of extracellular matrix, regulating various processes, including chronic inflammation, metastasis and embryonic implantation. MMP-3 (MT3-MMP; MMP-16) in addition to being fibroblast-associated, it is also involved in the regulation of MMP-2 and in direct matrix turnover, and is also widely expressed and capable of degrading several extracellular matrix components, including type I and III collagen (23-25). Therefore, it was hypothesized that miR-146b-5p may affect the expression of its target, MMP-16, and thus increase collagen fibers to result in hypertrophy of Osborne's ligament. miR-21-3p has been found to act as a fibroblast exosomal-derived miRNA, which can induce cardiomyocyte hypertrophy through silencing of its targets, sorbin and SH3 domain containing 2 or PDZ and LIM domain 5 (26). Furthermore, miR-21-3p has previously been reported to be associated with the diagnosis of fibromyalgia (27). Therefore, fibroblast-derived miR-21-3p may be involved in the hypertrophy of Osborne's ligament. The present study is the first, to the best of our knowledge, to identify the association between the three miRNAs (hsa-miR-1343-3p, hsa-miR-21-3p and hsa-miR-146-5p) and hypertrophy of Osborne's ligament, which may provide novel clues in investigations of hypertrophy of Osborne's ligament.

According to the results of the GO analysis in the present study, the predicted target genes were involved in protein metabolic process, regulation of cell growth, cell cycle process, regulation of cell division, cellular metabolic process and signal transmission, among others. These biological processes are likely to be important for the development of hypertrophy of Osborne's ligament. KEGG pathway analysis showed that CAMs, the MAPK signaling pathway, retrograde endocannabinoid signaling, the ErbB signaling pathway, glycosaminoglycan biosynthesis-heparin sulfate/heparin and the neurotrophic signaling pathway were among the most relevant pathways for the predicted target genes. Certain signaling pathways of these may be important in the pachyntic mechanism of Osborne's ligament, and these results provide a novel theoretical foundation for identifying potential therapeutic targets for CuTS.

TGF-β is a member of a large family of disulfide-bonded cytokines. The TGF-β superfamily members include TGF-β1-3, activin, nodal, bone morphogenetic protein (BMP)-2, -4 and -7, anti-Müllerian hormone/Müllerian inhibiting substance (AMH/MIS) and growth differentiation factor (GDF) 5. The TGF-β superfamily members signal through a unique pair of transmembrane serine-threonine kinases, known as type I and type II receptors, to mediate intracellular small mothers against decapentaplegic (Smad) signaling. The TGF-β/activin/nodal subfamily binds to ALK4, 5 and 7, and activates Smad2/ 3; whereas the BMP/GDF/MIS subfamily generally binds to ALK1, 2, 3 or 6, and activates Smad1/5/8. Activated Smad2/3 and Smad1/5/8 form a complex with Smad4 and enter the nucleus, where they regulate target gene expression. TGFβ1 signaling has previously been reported to be associated with tissue fibrosis, wound healing and scarring in humans (28-30). In addition, the overexpression of miR-146b-5p can decrease levels of SMAD4 by disrupting TGF-β signal transduction in thyroid cancer (31). These findings, together with those of the present study, support the hypothesis that TGFβ1/Smad signaling may be key in the pathogenesis of pachyntic Osborne's ligament and potential therapeutic targets of CuTS, even though this signaling pathway was not predicted by KEGG analysis.

As it is not possible to obtain normal Osborne's ligaments from healthy individuals, normal tendinous tissues around the two heads of the flexor carpi ulnaris were collected in patients with CuTS in the present study. It was not possible to confirm that the normal control tissues were entirely normal tendinous tissues. The majority of patients with degenerative ulnar neuritis have different degrees of elbow joint degeneration; therefore, the soft tissues around the bone structure, particularly the tendon, are likely to be degenerated, and this remains to be clarified. These clinical limitations may have affected the experimental results of the present study. In addition, the prediction of miRNA targets by biological analysis alone is insufficient and further experiments are required to verify predicted miRNA targets, for example through the use of miRNA transfection/knockdown and luciferase assays. Therefore, future investigations aim to perform these experiments to confirm the predicted miRNA targets in present study. The identification of the function of the differentially expressed miRNAs and their corresponding predicted target genes is likely to contribute to current understanding of hypertrophy of Osborne's ligament.

In conclusion, the miRNA expression profiles of the pachyntic Osborne's ligaments in patients with CuTS were significantly different, compared with those of control tendinous tissues. Altered miRNAs may lead to the excessive activation or inactivation of signaling pathways in Osborne's ligament. The present study also indicated that differentially expressed miRNAs may be involved in the pathogenesis of CuTS and provided a theoretical foundation for identifying novel clinical treatments for CuTS. The etiology of CuTS is complex and remains to be fully elucidated, however, the present study on the miRNAs of pachyntic Osborne's ligaments provided novel information for revealing the pathogenesis and pathology of CuTS.

Acknowledgements

This study was supported by the State Program of National Natural Science Foundation of China (grant no. 81371957), the State Key Program of the National Natural Science Foundation of China (grant no. 81330042), the Special Program for Sino-Russian Joint Research sponsored by the Ministry of Science and Technology, China (grant no. 2014DFR31210) and the Key Program sponsored by the Tianjin Science and Technology Committee, China (grant nos. 13RCGFSY19000 and 14ZCZDSY00044).

References

1. Wojewnik B and Bindra R: Cubital tunnel syndrome-Review of current literature on causes, diagnosis and treatment. J Hand Microsurg 1: 76-81, 2009.
2. Mondelli M, Giannini F, Ballerini M, Ginanneschi F and Martorelli E: Incidence of ulnar neuropathy at the elbow in the province of Siena (Italy). J Neurol Sci 234: 5-10, 2005.
3. Ilker U, Derya B, Ozay O, Orman C and Akan M: Ulnar nerve compression at the elbow caused by the epitrochleoanconeus muscle: A case report and surgical approach. Turk Neurosurg 24: 266-271, 2014.
4. Assmus H, Antoniadis G, Bischoff C, Hoffmann R, Martini AK, Preissler P, Scheglmann K, Schwerdtfeger K, Wessels KD and Wüstner-Hofmann M: Cubital tunnel syndrome - a review and management guidelines. Cent Eur Neurosurg 72: 90-98, 2011.
5. Shah CM, Calfee RP, Gelberman RH and Goldfarb CA: Outcomes of rigid night splinting and activity modification in the treatment of cubital tunnel syndrome. J Hand Surg Am 38: 1125-1130 e1, 2013.
6. Choi CK, Lee HS, Kwon JY and Lee WJ: Clinical implications of real-time visualized ultrasound-guided injection for the treatment of ulnar neuropathy at the elbow: A pilot study. Ann Rehabil Med 39: 176-182, 2015.
7. Bacle G, Marteau E, Freslon M, Desmoineaux P, Saint-Cast Y, Lancigu R, Kerjean Y, Vernet E, Fournier J, Corcia P, *et al*: Cubital tunnel syndrome: Comparative results of a multicenter study of 4 surgical techniques with a mean follow-up of 92 months. Orthop Traumatol Surg Res 100 (4 Suppl): S205-S208, 2014.
8. Liu CH, Chen CX, Xu J, Wang HL, Ke XB, Zhuang ZY, Lai ZL, Wu ZQ and Lin Q: Anterior subcutaneous versus submuscular transposition of the ulnar nerve for cubital tunnel syndrome: A systematic review and meta-analysis. PLoS One 10: e0130843, 2015.
9. Brown JM, Mokhtee D, Evangelista MS and Mackinnon SE: Scratch collapse test localizes osborne's Band as the point of maximal nerve compression in cubital tunnel syndrome. Hand (N Y) 5: 141-147, 2010.
10. Bartel DP: MicroRNAs: Genomics, biogenesis, mechanism, and function. Cell 116: 281-297, 2004.
11. Chen J, Liu Z, Zhong G, Qian L, Li Z, Qiao Z, Chen B and Wang H: Hypertrophy of ligamentum flavum in lumbar spine stenosis is associated with increased miR-155 level. Dis Markers 2014: 786543, 2014.
12. Dweep H and Gretz N: miRWalk2.0: A comprehensive atlas of microRNA-target interactions. Nat Methods 12: 697, 2015.
13. Livak KJ and Schmittgen TD: Analysis of relative gene expression data using real-time quantitative PCR and the 2(-Delta Delta C(T)) Method. Methods 25: 402-408, 2001.
14. Naran S, Imbriglia JR, Bilonick RA, Taieb A and Wollstein R: A demographic analysis of cubital tunnel syndrome. Ann Plast Surg 64: 177-179, 2010.
15. Descatha A, Leclerc A, Chastang JF and Roquelaure Y; Study Group on Repetitive Work: Incidence of ulnar nerve entrapment at the elbow in repetitive work. Scand J Work Environ Health 30: 234-240, 2004.
16. Gras C, Ratuszny D, Hadamitzky C, Zhang H, Blasczyk R and Figueiredo C: miR-145 contributes to hypertrophic scarring of the skin by inducing myofibroblast activity. Mol Med 21: 296-304, 2015.
17. Zhu H, Luo H, Li Y, Zhou Y, Jiang Y, Chai J, Xiao X, You Y and Zuo X: MicroRNA-21 in scleroderma fibrosis and its function in TGF-β-regulated fibrosis-related genes expression. J Clin Immunol 33: 1100-1109, 2013.
18. Li P, He QY and Luo CQ: Overexpression of miR-200b inhibits the cell proliferation and promotes apoptosis of human hypertrophic scar fibroblasts in vitro. J Dermatol 41: 903-911, 2014.
19. Geraldo MV, Fuziwara CS, Friguglieti CU, Costa RB, Kulcsar MA, Yamashita AS and Kimura ET: MicroRNAs miR-146-5p and let-7f as prognostic tools for aggressive papillary thyroid carcinoma: A case report. Arq Bras Endocrinol Metabol 56: 552-557, 2012.
20. Lin F, Wang X, Jie Z, Hong X, Li X, Wang M and Yu Y: Inhibitory effects of miR-146b-5p on cell migration and invasion of pancreatic cancer by targeting MMP16. J Huazhong Univ Sci Technolog Med Sci 31: 509-514, 2011.
21. Li Y, Wang Y, Yu L, Sun C, Cheng D, Yu S, Wang Q, Yan Y, Kang C, Jin S, *et al*: miR-146b-5p inhibits glioma migration and invasion by targeting MMP16. Cancer Lett 339: 260-269, 2013.
22. Simsek S, Er U, Demirci A and Sorar M: Operative illustrations of the Osborne's ligament. Turk Neurosurg 21: 269-270, 2011.
23. Jung JC, Wang PX, Zhang G, Ezura Y, Fini ME and Birk DE: Collagen fibril growth during chicken tendon development: Matrix metalloproteinase-2 and its activation. Cell Tissue Res 336: 79-89, 2009.
24. Van Doren SR: Matrix metalloproteinase interactions with collagen and elastin. Matrix Biol 44-46: 224-231, 2015.
25. Singh D, Srivastava SK, Chaudhuri TK and Upadhyay G: Multifaceted role of matrix metalloproteinases (MMPs). Front Mol Biosci 2: 19, 2015.
26. Bang C, Batkai S, Dangwal S, Gupta SK, Foinquinos A, Holzmann A, Just A, Remke J, Zimmer K, Zeug A, *et al*: Cardiac fibroblast-derived microRNA passenger strand-enriched exosomes mediate cardiomyocyte hypertrophy. J Clin Invest 124: 2136-2146, 2014.
27. Cerdá-Olmedo G, Mena-Durán AV, Monsalve V and Oltra E: Identification of a microrna signature for the diagnosis of fibromyalgia. PLoS One 10: e0121903, 2015.
28. Miyazono K, Suzuki H and Imamura T: Regulation of TGF-beta signaling and its roles in progression of tumors. Cancer Sci 94: 230-234, 2003.
29. Kamato D, Burch ML, Piva TJ, Rezaei HB, Rostam MA, Xu S, Zheng W, Little PJ and Osman N: Transforming growth factor-β signalling: Role and consequences of Smad linker region phosphorylation. Cell Signal 25: 2017-2024, 2013.
30. Finnson KW, Mclean S, Di Guglielmo GM and Philip A: Dynamics of transforming growth factor beta signaling in wound healing and scarring. Adv Wound Care (New Rochelle) 2: 195-214, 2013.
31. Geraldo MV, Yamashita AS and Kimura ET: MicroRNA miR-146b-5p regulates signal transduction of TGF-β by repressing SMAD4 in thyroid cancer. Oncogene 31: 1910-1922, 2012.